

## Spectral Characteristics of Bicalutamide Drug in Different Solvents and $\beta$ -Cyclodextrin

A. ANTON SMITH<sup>1</sup>, K. KANNAN<sup>1</sup>, R. MANAVALAN<sup>1</sup> and N. RAJENDIRAN<sup>1,2,\*</sup>

<sup>1</sup>Department of Pharmacy, Annamalai University, Annamalainagar, Chidambaram, 608 002, Tamil Nadu, India;

<sup>2</sup>Department of Chemistry, Annamalai University, Annamalainagar, Chidambaram, 608 002, Tamil Nadu, India

(Received: 4 February 2006; in final form: 28 July 2006)

**Key words:** bicalutamide,  $\beta$ -cyclodextrin, ICT, solvent effects

### Abstract

Absorption and fluorescence spectra of bicalutamide (BCA) in different solvents and aqueous  $\beta$ -cyclodextrin ( $\beta$ -CD) solutions are reported. The solid inclusion complex of BCA with  $\beta$ -CD is prepared and investigated by FT-IR, <sup>1</sup>H NMR, differential scanning calorimetry (DSC) and scanning electron microscopy (SEM). The Stokes shift of BCA is correlated with various solvent polarity scales like  $E_T(30)$ , BK and  $f(D,n)$ .  $\beta$ -CD studies show that (i) the absorption and emission maxima of BCA are shifted to red, (ii) the absorbance is slightly decreased whereas emission intensity is increased largely with an increasing  $\beta$ -CD concentration, (iii) BCA forms 1:1 inclusion complex with  $\beta$ -CD and (iv) intramolecular charge transfer (ICT) emission is present in the excited state.

### Introduction

A drug molecule in its electronically excited state has different electronic charge distribution at various atomic centers in comparison to that of the ground state and as a result its physical and chemical properties would differ from those in the ground state. Hence, the study of photochemical and photophysical process of drug molecules has always been of spectral interest to chemist [1–15] and pharmacists [3, 4].

Medicinal chemistry is concerned with the understanding of chemical and biological mechanism by which the action of drug molecules can be explained [1–4]. It also tries to establish relations between chemical structure and biological activity and to link the latter to the physical properties of the drug molecules. The discovery of a new and biologically important active compound usually gives rise to an extended search for closely related compounds of similar more effective, more specific or even opposite activity [15–17]. In many cases substitution of one atom or group of atoms in the parent compound (drug) results to surprising actions.

In recent years,  $\beta$ -CDs have been shown to be interesting micro vessels for several molecules and the resulting supramolecular species serve as excellent miniature models for enzyme substrate complexes [15–17]. The reduced polarity and the restricted space provided by the  $\beta$ -CD cavity markedly influence by a number of photophysical properties of the drug molecules. In

addition, especially in pharmaceutical industries, the inclusion process of drug molecules to  $\beta$ -CDs leads to important modifications of pharmaceutical properties of drug molecules. For example, the pharmaceutical interest in  $\beta$ -CDs extends to enhance solubility, chemical stability and bioavailability of poorly soluble drugs, to reduce toxicity and to control the rate of release [16]. The size of the  $\beta$ -CD and the drug molecule plays an important role to determine the complex type or stoichiometry. The drug can be present in the different parts of the  $\beta$ -CD depending on the type of inclusion complex formed. The reason for choosing  $\beta$ -CD is that the bicalutamide (BCA, (I)-*N*-[4-cyano-3-(trifluoromethyl)phenyl]-3-[(4-fluorophenyl)sulfonyl]-2-hydroxy-2-methyl propanamide, drug is quite large and thus it will orientate only lengthwise to the  $\beta$ -CD cavity. BCA is used as nonsteroidal antiandrogens for prostate cancer treatment [17].

### Experimental

#### Reagents

BCA was obtained from Cipla Ltd. pharmaceutical drug manufacturing company.  $\beta$ -CD and spectrograde solvents were purchased from E-Merck chemical company. The purity of the drug was checked by similar fluorescence spectra when excited with different wavelengths. Double distilled water was used for the preparation of aqueous solutions. The solutions were prepared just

\* Author for Correspondence. E-mail: drrajendiran@rediffmail.com

before taking measurements. The concentrations of the solutions were of the order  $2 \times 10^{-4}$  to  $2 \times 10^{-5}$  M. The concentration of  $\beta$ -CD is varied from  $1 \times 10^{-3}$  to  $1 \times 10^{-2}$  M.

#### Preparation of solid inclusion complex

Accurately weighed out 1.2 g of  $\beta$ -CD, were placed into a 50 ml conical flask and 30 ml of distilled water was added. 0.4 g of BCA was put into a 250 ml beaker and 20 ml methanol was added. Then  $\beta$ -CD solution was poured into the BCA solution and the resulting solution was continuously sonicated for 48 h at room temperature prior to being placed into a refrigerator for 24 h. At this time a white precipitate was formed which was filtered and washed with distilled water. The precipitate was dried in oven at  $60^\circ\text{C}$  for 12 h. This white precipitate an inclusion was characterized to be an complex of BCA with  $\beta$ -CD.

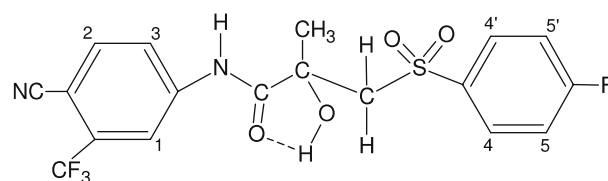
#### Instruments

Absorption spectral measurements were carried out with a Shimadzu UV 1601 PC model UV-visible spectrophotometer and the fluorescence measurements were made using a Perkin Elmer LS 55 spectrofluorimeter. FT-IR spectra were obtained with Avatar-330 FT-IR spectrometer using KBr pellet. The region covered was from 500 to  $4000\text{ cm}^{-1}$ . Bruker Advance DRX-400 MHz NMR spectrophotometer was used to study  $^1\text{H}$  NMR spectra. Microscopic morphological structure measurements were performed with a JEOL JSM 5610 LV scanning electron microscope (SEM) and a Shimadzu-60 differential scanning calorimeter (DSC) was used to measure the thermal curves.

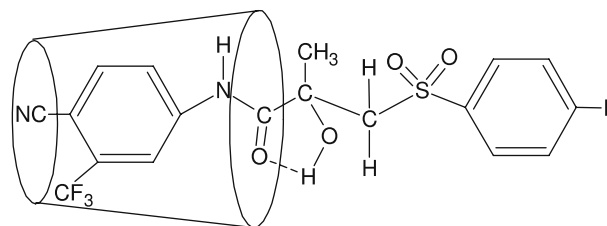
## Results and discussion

#### Effect of solvents

The absorption and fluorescence spectra of BCA (Scheme 1) NH have been observed in solvents of various polarities and hydrogen bonding capabilities. The relevant data for BCA are compiled in Table 1. The absorption spectra red shifted from cyclohexane to methanol. Solvents can interact with  $\text{C} \equiv \text{N}$  or NH or  $\text{C}=\text{O}$  groups. The interaction of solvents with the lone pair of the NH group will lead to a blue shift and the solvents with hydrogen atom of the NH group or lone pair of  $\text{C}=\text{O}/\text{C} \equiv \text{N}$  group will lead to a red shift both in absorption and fluorescence [18–20]. The red shift observed in the absorption spectrum is going from cyclohexane to water is due to the dispersive interactions of the aprotic and protic solvents, however water can act as proton donor and thus produce a blue shift (compared to methanol) in the absorption spectrum. This shows that the interaction of the NH group is large when compared to the  $\text{C} \equiv \text{N}/\text{C}=\text{O}$  groups. Fluorescence spectra of



BCA (by AM 1 method)



BCA- $\beta$ -CD

Scheme 1. Proposed structure of BCA- $\beta$ -CD inclusion complex.

BCA is red shifted from cyclohexane to water. A regular red shift is observed in the fluorescence spectra of BCA molecule with an increase in the solvent polarity indicates, the increase in the delocalization of the lone pair of electrons of the NH group throughout the aromatic ring in the  $S_1$  state. BCA gives two emission maxima in nonpolar cyclohexane, whereas it gives single emission maxima in other solvents (discussed in  $\beta$ -CD).

When a solute is placed in a solvent, one observes the combined effects of general and specific interactions. The separation of these interactions is often difficult. Theoretically derived solvent parameters like Reichardt's–Dimroth  $E_T(30)$  [21], Bilot–Kawski (BK) [22] and Lippert  $f(D,n)$  [23] values are accurate registers of solvent polarity have been used by several authors to correlate molecular spectroscopic properties [24]. Among these parameters BK and  $f(D,n)$  takes into account the solvents polarity alone, whereas  $E_T(30)$  incorporates both solvent polarity and hydrogen bonding effects. From the correlation of Stokes shifts with these parameters give an idea of about the type of interactions exerted between the solute and solvent can be obtained.

The solvatochromic shifts reveal that the hydrogen bonding interactions are present along with dipole interactions. In order to confirm this, we used the above parameters to correlate with Stokes shift of BCA molecule (Table 1). Figure 1 shows the plots of Stokes shift ( $\Delta \bar{\nu}_{ss}$ ) versus the  $E_T(30)$ , BK and  $f(D,n)$  parameters. The increase in  $\Delta \bar{\nu}_{ss}$  from cyclohexane to water in BCA is found to be more in accordance with  $E_T(30)$  than with BK and  $f(D,n)$  parameters. This is due to the hydrogen bonding interactions which are predominant in the solvatochromic shifts of BCA, hence  $\Delta \bar{\nu}_{ss}$  versus  $E_T(30)$  gives better correlation than the other two parameters.

#### Effect of $\beta$ -CD with BCA

Table 2 represents the absorption and emission maxima of BCA ( $2 \times 10^{-5}$  M) in aqueous solution (pH  $\sim$ 7)

Table 1. Absorption, fluorescence spectral data (nm) and Stokes shift ( $\text{cm}^{-1}$ ) of BCA in different solvents

S. no.	Solvents	$\lambda_{\text{abs}}$	$\lambda_{\text{flu}}$	Stokes shift
1.	Cyclohexane	267	320	6203
		215	285	
2.	Diethyl ether	270	322	5974
		218		
3.	1,4-Dioxane	271	325	6130
		216		
4.	Acetonitrile	271	326	6225
		216		
5.	Ethyl acetate	271	325	6130
		217		
6.	Dichloro methane	270	325	6300
		218		
7.	<i>t</i> -Butyl alcohol	272	331	6488
		215		
8.	2-Butanol	272	331	6488
		215		
9.	2-Propanol	272	331	6488
		216		
10.	1-Butanol	272	331	6488
		216		
11.	Ethanol	272	331	6488
		216		
12.	Methanol	272	331	6488
		216		
13.	Water	270	332	6909
		210		
Correlation co-efficient				
a. $E_T(30)$ versus $\Delta \bar{\nu}_{\text{SS}}$		0.8876		
b. BK versus $\Delta \bar{\nu}_{\text{SS}}$		0.6166		
c. $f(D,n)$ versus $\Delta \bar{\nu}_{\text{SS}}$		0.5947		

containing different concentration of  $\beta$ -CD. In  $\beta$ -CD free solution, the absorption maxima of BCA appears at 270 and 216 nm. Upon increasing the  $\beta$ -CD concentra-

tion, the absorption maxima is slightly red shifted to 274 and 219 nm. It has also been observed that, absorbance slightly decreases with increasing  $\beta$ -CD concentration. The above results are due to BCA molecule is transferred from more protic environments (bulk aqueous phase) to less protic environments ( $\beta$ -CD cavity). A clear isosbestic point at about 265 nm is observed in the absorption spectrum of BCA, indicating the formation of a 1:1 inclusion complex between BCA and  $\beta$ -CD.

For  $\beta$ -CD inclusion complexes, two parameters, i.e., the host-guest formation constant and the stoichiometry, have an important influence on the properties of the

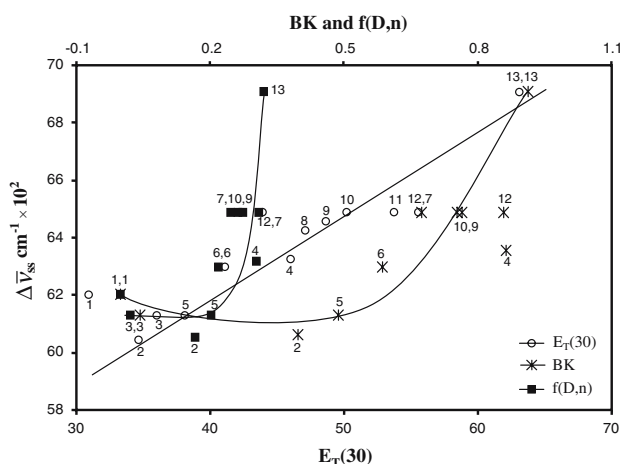


Figure 1. Plot of Stokes shifts ( $\text{cm}^{-1}$ ) of BCA versus  $E_T(30)$ , BK and  $f(D,n)$  solvent parameters: 1. cyclohexane, 2. diethyl ether, 3. 1,4-dioxane, 4. acetonitrile, 5. ethyl acetate, 6. dichloro methane, 7. *t*-butyl alcohol, 8. 2-butanol, 9. 2-propanol, 10. 1-butanol, 11. ethanol, 12. methanol, 13. water.

Table 2. Absorption and fluorescence maxima (nm) of BCA in different concentration of  $\beta$ -CD

Concentration of $\beta$ -CD ( $\text{M}$ ) $\times 10^{-3}$	$\lambda_{\text{abs}}$	$\lambda_{\text{flu}}$
0	270.0	328.4
1	271.0	329.0
5	273.0	329.6
10	274.0	330.8
$K$ ( $\text{M}^{-1}$ )	1364	2242
$\Delta G$ ( $\text{kJ mol}^{-1}$ )	-18.64	-19.44

included guest. There are several reported methods for processing the absorbance/fluorescence rate of  $\beta$ -CD host-guest systems [25] of which the double reciprocal plot [26], i.e., the reciprocal of the absorbance/fluorescence intensity of the  $\beta$ -CD inclusion complex versus the reciprocal of  $\beta$ -CD concentration is excellent, because the formation constant and stoichiometry can be simultaneously obtained from one plot.

For 1:1 inclusion complex between BCA and  $\beta$ -CD the following equilibrium can be written:



The formation constant ( $K$ ) and stoichiometric ratio of the inclusion complex of guest (BCA) can be determined according to the Benesi-Hildebrand [27] relation assuming the formation of a 1:1 BCA:  $\beta$ -CD complex is

$$1/\Delta A = 1/\Delta E + 1/K [\text{BCA}]_0 \Delta E \cdot [\beta\text{-CD}]_0 \quad (2)$$

where  $\Delta A$  is the difference between the absorbance of BCA in the presence and absence of  $\beta$ -CD,  $\Delta E$  is the difference between the molar absorption coefficient of  $\beta$ -CD and the inclusion complex,  $[\text{BCA}]_0$  and  $[\beta\text{-CD}]_0$  are the initial concentration of BCA and  $\beta$ -CD respectively. Figure 2 depicts a plot of  $1/\Delta A$  as a function of  $1/[\beta\text{-CD}]$  for BCA molecule. Good correlations were obtained confirming the formation of a 1:1 complex, the  $K$  value is calculated from the intercept and slope of the plot ( $K = 1634 \text{ M}^{-1}$ ).

As like in absorption, the fluorescence spectra of the BCA molecule undergo a slight red shift (328–331 nm) with increasing  $\beta$ -CD concentration (Table 2, Figure 3). However the fluorescence intensity is increased upon addition of  $\beta$ -CD. The enhancement of the fluorescence intensity in the BCA is due to the formation of a BCA- $\beta$ -CD inclusion complex. On formation of a BCA- $\beta$ -CD inclusion complex, the BCA molecule is encapsulated in the nonpolar  $\beta$ -CD cavity and experiences a nonpolar microenvironment. Thus, the bathochromic shift of the fluorescence maximum of BCA is observed with an in-

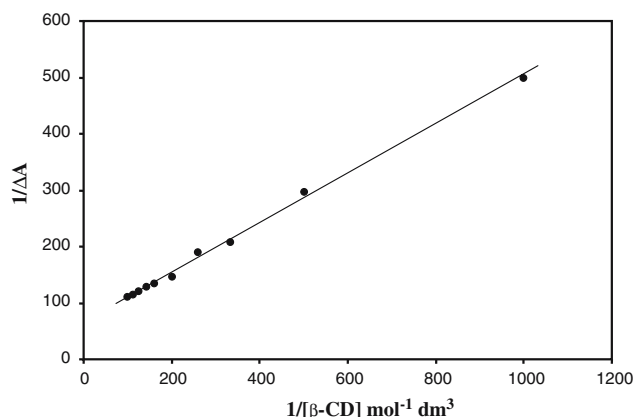


Figure 2. Benesi-Hildebrand plot of  $1/\Delta A$  versus  $1/[\beta\text{-CD}]$  for BCA.

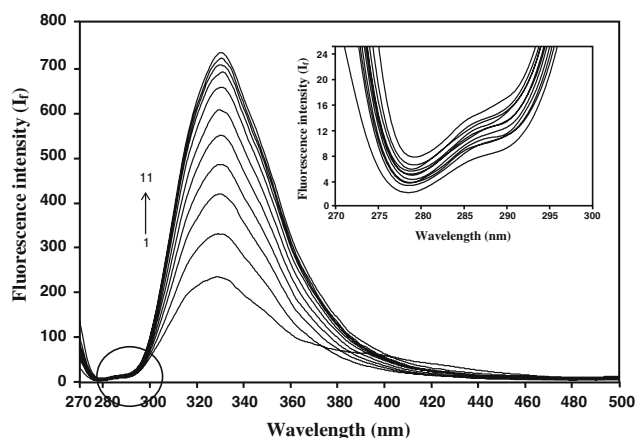


Figure 3. Fluorescence spectra of BCA in different  $\beta$ -CD concentrations ( $\text{mol dm}^{-3}$ ): 1. 0, 2. 0.001, 3. 0.002, 4. 0.003, 5. 0.004, 6. 0.005, 7. 0.006, 8. 0.007, 9. 0.008, 10. 0.009, 11. 0.010. Insert figure: Expansion of 285 nm maxima.

crease in  $\beta$ -CD concentration (Figure 3). As previously observed accommodation of fluorescence guest by  $\beta$ -CD enhances the fluorescence intensity [28]. Hence, the increase in the fluorescence intensity and bandwidth of the BCA molecule recorded in  $\beta$ -CD suggest the formation of a 1:1 inclusion complex of this molecule. The complexation is completed at  $7 \times 10^{-3} \text{ M}$   $\beta$ -CD concentration. There is no significant change in the fluorescence intensity in BCA molecule by further addition of  $\beta$ -CD. As like in absorption, the formation constant value is determined from the slope and the intercept of the plot (Figure 4). This formation constant ( $K = 2242 \text{ M}^{-1}$ ) value in fluorescence is greater than that obtained from the absorption, because the change in fluorescence intensity upon addition of  $\beta$ -CD is significantly greater than the absorption.

The free energy can be calculated from the constant, by the following equation

$$\Delta G = -RT \ln K \quad (3)$$

$\Delta G$  is negative suggesting that the inclusion process proceeded simultaneously at 303 K (Table 2).

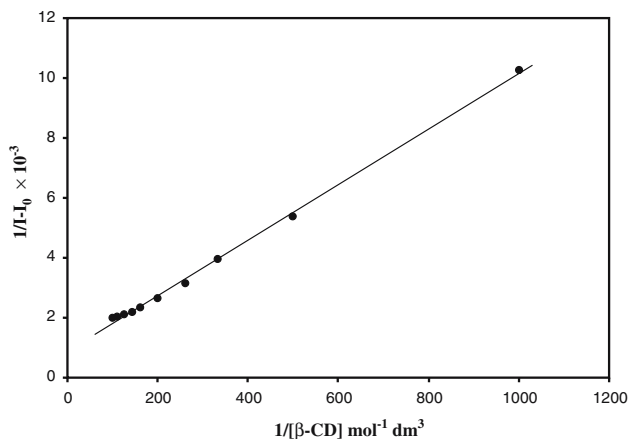


Figure 4. Benesi-Hildebrand plot of BCA with  $\beta$ -CD (Plot of  $1/I - I_0$  versus  $1/[\beta\text{-CD}]$ ).

A considerable increase in the fluorescence intensity compared with the nearly constant absorbance or slight decrease means that intramolecular charge transfer (ICT) emission of BCA is increased in the presence of  $\beta$ -CD (Figure 3). For example, the fluorescence intensity of BCA in the presence of  $1 \times 10^{-2}$   $\beta$ -CD is 4 times greater than that in the absence of  $\beta$ -CD. It should be noted that such a comparison is significant because of the small shift in the fluorescence and absorption spectra. A similar characteristics is also observed in various fluorophores by Jiang *et al.* [28a], Nag and Bhattacharaya [29] and Samanta *et al.* [30]. Large Stokes shift observed in all solvents and two emissions are observed in water (285 and 325 nm) further supported this implication.

Usually large red shift is observed in ICT molecule. However, a small red shift observed in BCA molecule is explained as follows: electron donating group present in between two electron withdrawing groups (C=O and C $\equiv$ N). These two groups prevent complete charge transfer from NH group, which hindered the ICT emission. The carbonyl group present adjacent to NH group effectively withdraw the electrons from the NH group. This hindered the effective delocalization between C $\equiv$ N and NH group. The small spectral shifts observed in solvents and  $\beta$ -CD (Table 1) may serve as further evidence to this conclusion, since the spectral shift directions of normal state and ICT state are opposite to each other. In the inclusion complex, the cyano group is present in the interior part of the  $\beta$ -CD activity, reducing the polarity of the cyano group, hence ICT emission intensity is increased in the  $\beta$ -CD solutions (Scheme 1). Due to the high polarity of water compared with organic solvents, ICT state is strongly solvated in aqueous solution; the fluorescence of ICT state is quenched because of the appreciable radiation less decay and intersystem crossing. Therefore the ICT state of BCA is mainly present in the less polar medium. Due to ICT emission, a large Stokes shift is observed in nonpolar cyclohexane solvent and the full width and half a maximum (FWHM) is increases from nonpolar solvent to water.

#### FT-IR spectral studies

The FTIR spectra of BCA nitrile group is characterised by weak absorption in the triple bond stretching  $2230 \text{ cm}^{-1}$ . The  $\text{CF}_3$  group absorb strongly at  $1328 \text{ cm}^{-1}$ . BCA molecule which incorporates group show stretching absorption in  $3338, 3465, 3577 \text{ cm}^{-1}$ . The C=O stretching and aromatic C-H stretching frequencies area at  $1690$  and  $3049 \text{ cm}^{-1}$  respectively. The above frequencies significantly changed in the inclusion complex i.e., C $\equiv$ N  $\sim 2235$ ,  $\text{CF}_3$   $\sim 1334, \sim 3341, 3672$  and C=O  $\sim 1695 \text{ cm}^{-1}$ . The  $\text{CF}_3$  deformation frequency is also significantly shifted in the inclusion complex  $510\text{--}643$  to  $500\text{--}635 \text{ cm}^{-1}$ . However, no significant change is observed in the  $\text{SO}_2$  symmetric, stretching ( $1137 \text{ cm}^{-1}$ ) and Ar-F stretching ( $1240 \text{ cm}^{-1}$ ) frequencies. The cyclodextrin peak is present only in the inclusion com-

Table 3.  $^1\text{H}$  NMR chemical shifts data of BCA and inclusion complex in  $\text{D}_2\text{O}$  containing 5% DMSO at  $20^\circ\text{C}$  (number assigned seen in Scheme 1)

	Pure BCA	Inclusion complex	$\Delta\delta$
NH	10.250	10.007	+0.243
OH	6.451	6.410	+0.041
$\text{CH}_2$	3.978	3.990	-0.022
$\text{CH}_3$	1.502	1.520	-0.018
$^1\text{H}$	8.390	8.328	+0.062
$^2\text{H}$	8.130	8.063	+0.067
$^3\text{H}$	7.854	7.830	+0.024
$^4\text{H}/^4\text{H}'$	7.927	7.940	-0.013
$^5\text{H}/^5\text{H}'$	7.212	7.227	+0.015

plex ( $2925 \text{ cm}^{-1}$ ). The above results indicate  $\text{CF}_3$ , C $\equiv$ N and NH groups are present in the  $\beta$ -CD cavity.

#### $^1\text{H}$ NMR spectral studies

$^1\text{H}$  NMR spectroscopy provides an effective means of assessing the dynamic interactions site of  $\beta$ -CD with that of the guest molecules [31]. The basis of information gained from NMR spectroscopy is located in this shifts, loss of resolution and broadening of signals observed for the  $\beta$ -CD and guest molecule protons. The addition of BCA to the  $\beta$ -CD solution results in a upfield shift for the part of the BCA drug protons chemical shifts in  $\text{D}_2\text{O}$  with 5% DMSO is given in Table 3. Due to poor solubility of the guest toward  $\text{D}_2\text{O}$ , we are forced to add atleast 5% of  $\text{DMSO-}d_6$  as a cosolvent. As can be seen from Table 3, the chemical shifts data for the inclusion complex was different from the free compound. In the inclusion complex, the BCA molecule NH,  $^1\text{H}$ ,  $^2\text{H}$  and  $^3\text{H}$  protons are largely upfield shift, which suggested that CN/ $\text{CF}_3$  aromatic ring is encapsulated in the  $\beta$ CD cavity.

#### Differential scanning calorimetry (DSC) study

The DSC curves of BCA,  $\beta$ -CD and inclusion complex are shown in Figure 5. From Figure 5, it can be shown that DSC curves of inclusion complex with the DSC curves of BCA and BCA- $\beta$ -CD is different from each

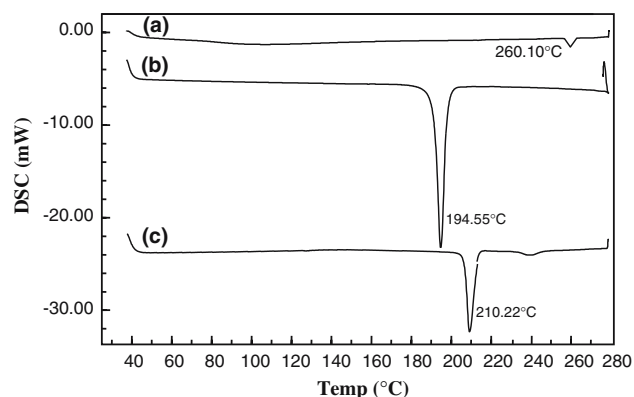


Figure 5. Thermal spectra of (a)  $\beta$ -CD, (b) BCA and (c) BCA- $\beta$ -CD inclusion complex.



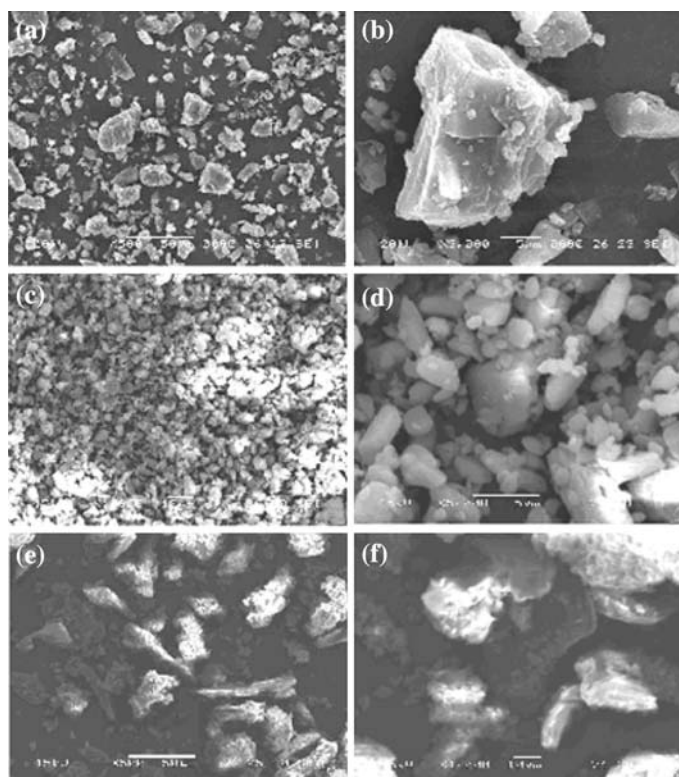


Figure 6. Scanning electron microscope photographs (Pt. coated) of (a)  $\beta$ -CD ( $\times 500$ ), (b)  $\beta$ -CD ( $\times 3000$ ), (c) BCA ( $\times 1000$ ), (d) BCA ( $\times 5000$ ) and (e and f) BCA- $\beta$ -CD inclusion complex ( $\times 500$  and  $\times 1000$ ).

other i.e.,  $\beta$ -CD  $\sim 260$  °C, time  $\sim 19.15$  min; BCA  $\sim 194$  °C, time  $\sim 16.46$  min; BCA- $\beta$ -CD  $\sim 210$  °C, time  $\sim 17.40$  min. These values prove that a new inclusion complex is formed.

#### Microscopic morphological observation

First we observed power form of BCA and  $\beta$ -CD by SEM and then we saw a powder form of the inclusion complex (Figure 6). As seen from the SEM figure, (i) pure  $\beta$ -CD is in platted form, (ii) BCA is present in smaller stones structure and (iii) inclusion complex is present in colloidal structure. These pictures clearly elucidated the difference in each case. Modification of crystals and powder can be assumed as a proof of the formation of new inclusion complex.

#### Acknowledgement

One of the author (N.R) is thankful to the Department of Science and Technology, New Delhi, for the financial support to the Project under Fast Track Proposal – Young Scientist Scheme No. SR/FTP/CS-14/2005 and University Grants Commission No. F-31-98/2005 (SR).

#### References

1. J.K. Dey and I.M. Warner: *J. Lumin.* **71**, 105 (1997); *J. Photochem. Photobiol. A: Chem.* **116**, 27 (1998); *J. Photochem. Photobiol. A: Chem.* **101**, 21 (1996).
2. G. Zhang, S. Shuang et al: *J. Photochem. Photobiol. A: Chem.* **169**, 153 (2005).
3. I.E. Borissevitch, and S.C.M. Gandini: *J. Photochem. Photobiol. B: Biol.* **43**, 112 (1998).
4. V.S. Chirvony, P.Y. Turpin et al: *J. Photochem. Photobiol. B: Biol.* **40**, 154 (1997).
5. Y.L. Wei, L.H. Ding, C. Dong, W.P. Niu, and S. Min Shuang: *Spectrochim. Acta* **59A**, 2697 (2003).
6. G. Fugen and L. Cuijing: *Chin. Pharm. J.* **33**, 153 (1998).
7. L. Xiyang and Y. Yunginf: *Chim. Pharm. J.* **32**, 218 (1997).
8. J.L. Manzoori and M. Amjadi: *Spectrochim. Acta* **59A**, 909 (2003).
9. I. Duran-Meras, A. de la Munoz pena, F. Salinas, and I. Rodriguez Caceres: *Analyst* **119**, 1251 (1994).
10. R.E. Galian, A.V. Veglia, and R.H. de Rossi: *Analyst* **123**, 1587 (1998).
11. G.M. Escandar: *Analyst* **124**, 587 (1999).
12. R.E. Galian, A.V. Veglia, and R.H. de Rossi: *Analyst* **125**, 1465 (2000).
13. S.S. Adams, P. Bresloff, and C.G. Mason: *J. Pharm. Pharmacol.* **28**, 256 (1976).
14. R. Canaparo, E. Mumtoni, G.P. Zara, C. Dellapena, E. Berno, M. Costa, and M. Endi: *Biomed. Chromatogr.* **14**, 219 (2000).
15. J.F. Li, Y.X. Wei, L.H. Ding, and C. Dong: *Spectrochim. Acta* **59A**, 2759 (2003).
16. (a) D.M. Brahmankar and S.B. Jaiswal: *Biopharmaceutics and Pharmacokinetics, A-Treastise*, Vallabh Prakasham Pubs., p. 302 (2006); (b) J. Chao, D. Meng, J. Li, H. Xi, and S. Huang: *Spectrochim. Acta*, **60A**, 729 (2004).
17. (a) D.A. William and T.C. Lenke: *Foye's Principle of Medicinal Chemistry*, 5th edn., B.I. Pubs., p. 711 (2005); (b) C.I. Carswell and P. Figgitt, *Drugs* **62**, 2471 (2002).
18. N. Rajendiran and M. Swaminathan: *Bull. Chem. Soc. Japan* **68**, 2997 (1995); *J. Photochem. Photobiol. A: Chem.* **93**, 109 (1996).
19. T. Stalin and N. Rajendiran: *Spectrochim. Acta*, **62A**, 991 (2005); *Spectrochim. Acta* **61A**, 3087 (2005); *Spectrochim. Acta* **61A**, 2495 (2005).
20. T. Stalin and N. Rajendiran: *J. Photochem. Photobiol. A: Chem.* **177**, 144 (2006); *Chem. Phys.* **322**, 311 (2006); *J. Incl. Phenom. Macrocyclic Chem.* **55**, 21 (2006); *J. Mol. Struct.* **794**, 35 (2006); *J. Photochem. Photobiol. A: Chem.* **182**, 137 (2006).
21. C. Reichardt and K. Dimroth: *Fortschr. Chem. Forsch.* **11**, 1 (1968).

22. L. Bilot and A Kowski: *Z. Naturforsch.* **18A**, 621 (1962).
23. E. Lippert: *Z. Naturforsch.* **10A**, 541 (1955); *Z. Electrochem.* **61**, 962 (1957).
24. M.K. Nayak and S.K. Dogra: *J. Photochem. Photobiol. A: Chem.* **161**, 169 (2004).
25. Y.B. Jiang and X.Z. Huang: *G.Z. Chem. Huaxue Tongbao* **9**, 46 (1990).
26. G.C. Catene and F.V. Bright: *Anal. Chem.* **61**, 905 (1986).
27. H.A. Benesi and J. Hildebrand: *J. Am. Chem. Soc.* **71**, 2703 (1949).
28. (a) Y.B. Jiang and X.J. Wang: *J. Photochem. Photobiol. A: Chem.* **81**, 205 (1994); (b) Y.H. Kim, D.W. Cho, and M. Yoon: *J. Phys. Chem.* **100**, 15670 (1996); (c) S. Panja and S. Chakravarti: *Chem. Phys. Lett.* **336**, 57 (2001); (d) S. Hamai and K. Hari: *Supramol. Chem.* **10**, 43 (1998).
29. A. Nag. K. Bhattacharya: *Chem. Phys. Lett.* **151**, 474 (1988); *J. Chem. Soc. Faraday Trans.* 86, 53 (1990).
30. T. Soujanya, T.S.R. Krishna, and A. Samanta: *J. Phys. Chem.* **96**, 8544 (1992); *J. Photochem. Photobiol. A: Chem.* **66**, 185 (1992).
31. J.B. Chao, H.B. Tong, S.P. Huang, and D.S. Lie: *Spectrochim. Acta* **60A**, 161 (2004); M.C. Rath, D.K. Palit, and T. Mukherjee: *J. Chem. Soc. Faraday Trans.* 94, 1189 (1998).